SPECIAL TOPIC — Smart design of materials and design of smart materials

Designing radiative cooling metamaterials for passive thermal management by particle swarm optimization

Shenshen Yan(闫申申)[1], Yan Liu(刘岩)[1], Zi Wang(王子)[1,†], Xiaohua Lan(兰晓华)[1], Yi Wang(汪毅)[1], and Jie Ren(任捷)[1,2,‡]

[1] *Center for Phononics and Thermal Energy Science, China-EU Joint Laboratory on Nanophononics, Shanghai Key Laboratory of Special Artificial Microstructure Materials and Technology, School of Physics Science and Engineering, Tongji University, Shanghai* 200092, *China*
[2] *Shanghai Research Institute for Intelligent Autonomous Systems, Tongji University, Shanghai* 200092, *China*

(Received 15 January 2023; revised manuscript received 10 February 2023; accepted manuscript online 2 March 2023)

The passive radiative cooling technology shows a great potential application on reducing the enormous global energy consumption. The multilayer metamaterials could enhance the radiative cooling performance. However, it is a challenge to design the radiative cooler. In this work, based on the particle swarm optimization (PSO) evolutionary algorithm, we develop an intelligent workflow in designing photonic radiative cooling metamaterials. Specifically, we design two 10-layer SiO_2 radiative coolers doped by cylindrical MgF_2 or air impurities, possessing high emissivity within the selective (8–13 μm) and broadband (8–25 μm) atmospheric transparency windows, respectively. Our two kinds of coolers demonstrate power density as high as 119 W/m^2 and 132 W/m^2 at the room temperature (300 K). Our scheme does not rely on the usage of special materials, forming high-performing metamaterials with conventional poor-performing components. This significant improvement of the emission spectra proves the effectiveness of our inverse design algorithm in boosting the discovery of high-performing functional metamaterials.

Keywords: photonic devices, passive radiative cooling, metamaterial, optimization algorithm

PACS: 78.67.Pt, 44.40.+a, 81.05.Zx **DOI:** 10.1088/1674-1056/acc061

1. Introduction

With the rapid development of modern industrialization, the traditional cooling technology consumes a large amount of energy source.[1,2] The passive radiative cooling technology without any external energy input has been regarded as a promising method in the field of energy science.[3–6] Based on the atmosphere transparent window in the wavelength range of 8–13 μm, the thermal radiation of terrestrial objects at the room temperature (300 K) holds peaks exactly in the atmospheric transparent window, which radiates the dissipated heat directly to the outer space.[7,8]

Nighttime radiative cooling has been extensively studied and successively implemented for decades.[9–17] However, the practical cooling tasks are usually during the daytime,[3,7,18–22] which are much more difficult due to the heating effect of the sunlight. The goals to achieve daytime radiative cooling are to minimize the absorption of sunlight and simultaneously enhance the emissivity of the device in the atmospheric transparent window.[3,7,22–25]

There are a series of excellent photonic materials proposed in the radiative cooling field,[26] e.g., multilayer structures,[3] metamaterials,[19] randomly distributed particle structures,[22] and porous structures.[27] The radiative cooling materials have many potential applications on energy-efficient buildings,[28–32] enhanced solar cells cooling,[33,34] cooling textiles,[35–37] electricity generation[38,39] and water harvesting.[40] These wide variety of photonic materials with different thermal performance provide a broad perspective for the manufacture of radiation cooling devices.

Recently, the great potential brought by the machine learning has ignited the field of material science and photonic device.[41–46] The machine learning is utilized to inversely design photonic crystal structures[47–49] and radiative coolers.[41,50–56] Moreover the multilayer photonic device with microstructures has been demonstrated as high-performing radiative cooling devices.[7,21,51,57–59] Therefore, the machine learning technology has the wide application prospects of designing the high-performing radiative cooling metamaterials.

In this work, we use SiO_2 with high emissivity in the atmospheric transparency window and MgF_2 as basic materials, taking advantages of their high sunlight transparency and therefore low daytime radiation absorption.

Based on the particle swarm optimization (PSO) algorithm, we design two kinds of high-performing photonic metamaterials for selective and broadband radiative cooling. The results show that the selective radiative cooler has the cooling power of 119 W/m^2 and the broadband one has a cooling power of 132 W/m^2 in the room temperature environment.

[†]Corresponding author. E-mail: prince@tongji.edu.cn
[‡]Corresponding author. E-mail: xonics@tongji.edu.cn

© 2023 Chinese Physical Society and IOP Publishing Ltd

Therefore, the two multi-layers microstructures could be used for the passive radiative cooling. And our photonic metamaterial design with the PSO algorithm shows the immense potential on exploring radiative coolers with higher cooling power and designing the high-performing functional photonic metamaterials.

2. Theory of radiative cooling

Generally, the daytime radiative cooler is mainly affected by solar thermal radiation, atmospheric and nonradiative (conductive and convective) heat exchange, as well as the surrounding air as shown in Fig. 1. Therefore, the net radiative cooling power P_c of the cooler is defined by[4,7]

$$P_c(T_c) = P_{rad}(T_c) - P_{atm}(T_{amb}) - P_{sun} - P_{nonrad}. \quad (1)$$

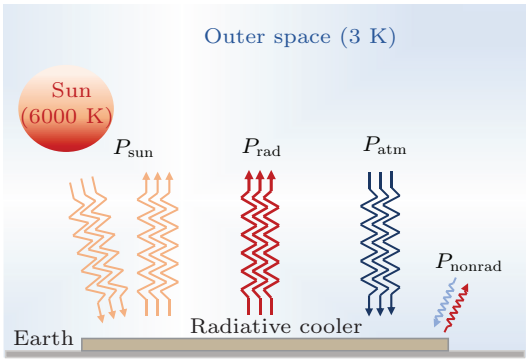


Fig. 1. Schematics of radiative and nonradiative heat exchange processes among radiative cooler, atmosphere and outer space. P_{rad}, P_{atm}, P_{sun} and P_{nonrad} are the power emitted from the radiative cooler, radiative power from atmosphere absorbed by the radiative cooler, solar power absorbed by radiative cooler and non-radiative heat exchange (conductive and convective) power, respectively.

The first item in Eq. (1) $P_{rad}(T_c)$ is the power emitted by the radiative cooler with area A which can be expressed as

$$P_{rad}(T_c) = A\int_0^{2\pi} d\phi \int_0^{\pi/2} \sin(\theta)\cos(\theta) d\theta \times \int_0^{\infty} I_{BB}(T_c,\lambda)\varepsilon(\lambda,\theta,\phi) d\lambda, \quad (2)$$

where T_c is the temperature of the radiative cooler, θ (ϕ) is the polar (azimuth) angles, $I_{BB}(T,\lambda) = \frac{2hc^2}{\lambda^5}\frac{1}{e^{hc/k_BT}-1}$ is the spectrum density of the black body at temperature T with h, c, λ and k_B being respectively the Planck's constant, the speed of light in vacuum, the wavelength and the Boltzmann constant. Here, $\varepsilon(\lambda,\theta,\phi)$ is the generally anisotropic emissivity of the radiative cooler, which hereafter is considered independent of ϕ.[4,7]

The second item in Eq. (1) $P_{atm}(T_{amb})$ is the radiative power from atmospheric absorbed by the radiative cooler,

$$P_{atm}(T_{amb}) = 2\pi A\int_0^{\pi/2} d\theta \sin(\theta)\cos(\theta) \times \int_0^{\infty} I_{BB}(T_{amb},\lambda)\varepsilon(\lambda,\theta)\varepsilon_{atm}(\lambda,\theta) d\lambda, \quad (3)$$

where T_{abm} is the temperature of the atmosphere, $\varepsilon_{atm} = 1 - t(\lambda)^{1/\cos(\theta)}$ is the angle dependent emissivity of atmosphere, and $t(\lambda)$ is the atmospheric transmittance in the zenith direction.

The third item in Eq. (1) P_{sun} is the solar power absorbed by the radiative cooler,

$$P_{sun} = A\int_0^{\infty} d\lambda I_{AM\ 1.5}(\lambda)\varepsilon(\lambda,\theta_{sun}), \quad (4)$$

where $I_{AM\ 1.5}(\lambda)$ is the solar illumination, and θ_{sun} is the fixed angle between the incident sunlight and the radiative cooler.

The last item in Eq. (1) P_{nonrad} represents the nonradiative heat heat exchange power of the cooler with the surrounding environment, which can be given by

$$P_{nonrad}(T_c,T_{amb}) = Ah(T_{amb} - T_c), \quad (5)$$

where $h = h_{cond} + h_{conv}$ is the total non-radiative heat coefficient combining heat conduction coefficient h_{cond} with heat convection coefficient h_{conv}.

As shown in Eq. (1), when the power emitted by the radiative cooler is lager than that absorbed from outer space, the cooling effect occurs. The temperature of cooler T_c will continue to decrease until the net cooling power is equal to zero, reaching a steady temperature T_{steady}. Therefore, to obtain the optimal cooling effect, one should simultaneously reduce the absorbed power and enhance the dissipative radiation in the atmospheric transparent window.

3. Inversely designing photonic metamaterials with evolutionary algorithm

The evolutionary algorithms show the great potential in inversely and efficiently designing the functional materials instead of the traditional trial-and-error method.[46,60,61] And the PSO algorithm is a kind of effective biological swarm intelligence algorithm, which has the advantages of easy implementation, few hyper-parameters, and fast convergence.[46,60,62,63] In this work, we develop a paradigm to systematically design the photonic metamaterials. As shown in Fig. 2, our framework mainly contains the stages of (i) the material definition, (ii) metamaterial configuration, (iii) fitness calculation and (iv) the evolution with PSO evolutionary algorithm.

The material definition as input parameters of the workflow needs to be prepared in advance, including the number of layers, the maximum thickness of each layer, the type of the microstructure units and the maximum number of the units in each layer. The optimization problem becomes increasingly difficult with the increment of structure complexity. Although, with more layers, more complex spectrum can be achieved in principle, the larger number of layers makes the searching space more complex and the spectrum calculations time-consuming. Here in this work, for tractability, we define (at most) 10 SiO_2 layers as the substrate. Because MgF_2 is

transparent over an extremely wide range of wavelength, it is widely used in the windows, lenses and radiative coolers.[7,41] The multilayer SiO_2 with MgF_2 and air units could take the advantages of their high sunlight transparency and therefore low daytime radiation absorption. With this motivation, our micro-cylinders are filled by air or MgF_2. We also restrict the centers of the cylinders in each SiO_2 layer to the same positions for the sake of model simplicity.

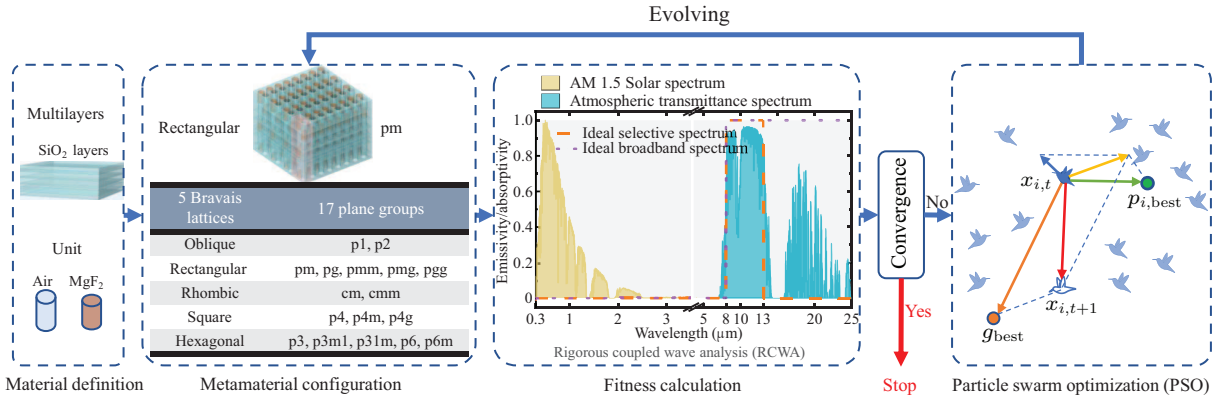


Fig. 2. Designing schematic of the radiative cooling metamaterials. The schematics mainly includes four parts, the material definition, metamaterial configurations, fitness calculation and evolution with particle swarm optimization (PSO). The schematics starts with the material definition as the input parameters which includes the materials, layers, and units. The material configuration will generate the metamaterials with the symmetry of the 17 plane groups. And the spectrum of the metamaterial is calculated by the RCWA in the fitness calculation part. The PSO part will make the population of metamaterials evolve towards the new metamaterials with the better radiative cooling performance until reaching convergence condition.

The metamaterial configuration comprises the thickness of each layer, 2D lattice parameters and center coordinate, radius and filled material of each cylinder. For the initialization, in the metamaterial configuration part, the thickness of each layer is randomly generated within the maximum thickness. Initially generating structures with consideration of the spatial symmetry ensures not only the unbiased sampling of the search space, but also higher diversity in the population of structures than the fully random initialization of structures.[60,64,65] Thus, in this work, the crystal metamaterials are randomly generated according to the plane group symmetries. The lattice parameters of the metamaterial belong to 5 Bravais lattices in the two-dimensional (2D) plane. The centers of the cylinders are regarded as the Wyckoff positions of the 17 2D plane groups.

The spectrum of layered photonic metamaterial is calculated by S^4 based on the rigorous coupled-wave analysis (RCWA) method.[66] The fitness function between the resulting spectrum $S_{\boldsymbol{x}}(\lambda)$ and the ideal spectrum $A(\lambda)$ is set as

$$F_{\boldsymbol{x}} = \int \mathrm{d}\lambda |A_{\boldsymbol{x}}(\lambda) - S_{\boldsymbol{x}}(\lambda)|, \tag{6}$$

where the vector $\boldsymbol{x}$ contains the configuration parameters of our metamaterial structure. The emissivity of the ideal selective (broadband) radiative cooler is $A(\lambda) = 1$ for $\lambda \in [8, 13]$ μm ($\lambda \in [8, 25]$ μm) and zero otherwise.

The designing of metamaterials is thus equivalent to minimizing Eq. (6). We utilize the PSO algorithm to make the whole population evolves towards the photonic metamaterial with less fitness as[62,67]

$$\begin{aligned} \boldsymbol{v}_{i,t+1} &= w_t \boldsymbol{v}_{i,t} + c_1 \boldsymbol{r}_1 \odot (\boldsymbol{p}_{i,\mathrm{best}} - \boldsymbol{x}_{i,t}) \\ &\quad + c_2 \boldsymbol{r}_2 \odot (\boldsymbol{g}_{\mathrm{best}} - \boldsymbol{x}_{i,t}), \\ \boldsymbol{x}_{i,t+1} &= \boldsymbol{x}_{i,t} + \boldsymbol{v}_{i,t+1}, \end{aligned} \tag{7}$$

where i represents the index of the metamaterial structure as well as particle, t is the number of iteration and $\odot$ is the Hadamard (elementwise) product, w_t is the inertia weight of the velocity vector of particle i $\boldsymbol{v}_{i,t}$, the acceleration constants c_1 and c_2 are equal to 2, and $\boldsymbol{r}_1$, $\boldsymbol{r}_2$ are the random vectors with elements in the range of $[0, 1]$. Here, $\boldsymbol{g}_{\mathrm{best}}$ is the global best photonic metamaterial, which corresponds to the material with the minimum of fitness during the whole design process and $\boldsymbol{p}_{i,\mathrm{best}}$ is the local best photonic metamaterial ever explored by particle i. The inertia weight is annealed linearly from 0.9 to 0.4 as $w_t = w_{\max} - (w_{\max} - w_{\min})/t_{\max} \cdot t$, with $t_{\max}$ being the maximum number of iterations.[67,68] The three parts of new velocity in Eq. (7) are also respectively called the inertia of the velocity, individual cognition and social knowledge sharing. Generally, the velocity of each particle in parameter space is stochastically accelerated towards its previous best metamaterial configuration (personal best) and towards the best solution of the population (global best) within the total 17 2D plane groups. Therefore, each metamaterial configuration is updated according to its new velocity without confining the symmetry. During the evolving process, in order to increase the diversity of the population, the worse 30% of the population metamaterial structures will be replaced by the initially generated metamaterials. When the convergence condition is reached, the evolutionary program will be terminated.

On one hand, an ideal selective radiative cooler emitting in the range of 8–13 μm could reach a lower steady-state temperature than an ideal broadband radiative cooler, due to its lower radiation absorption.[8] On the other hand, above

the ambient temperature, the power of an ideal cooler can be significantly enhanced by broadening its effective emission range.[3,8,20,69] Therefore, in this work, we consider both these two kinds of coolers with performance tradeoff, since they are possibly suitable for different working conditions. With our multilayer photonic metamaterial design workflow, we devise the two kinds of multilayer photonic metamaterials to cover the 8–13 μm and 8–25 μm atmospheric transparency window ranges as the selective and broadband radiative coolers, respectively.

4. Results and analysis

First of all, we design a selective radiative cooler. The goal is that the emissivity in the range 8–13 μm is 1, and the emissivity of other wavelength range is 0, as shown in Fig. 3(a) and Table 1. The selective radiative cooler is composed of 10 layers of SiO_2, which are stacked from top to bottom, and the thicknesses are 4.90, 4.11, 3.71, 0.41, 3.50, 1.57, 2.24, 4.72, 2.77, and 0.07 μm respectively. Each layer of SiO_2 film is embedded with MgF_2/air cylinders. The rectangle lattice of the primitive cell is 4.74 μm×8.76 μm with *pm* plane group symmetry. The center coordinates of each layer filled with circular holes are (0.0, −1.52 μm), (0.0, 1.52 μm) respectively. The radii of filled cylinders in one layer are the same and different in different layers, i.e., 1.45, 1.25, 1.20, 1.27, 1.40, 1.24, 1.44, 1.35, 1.16, 1.38 μm from the top to bottom.

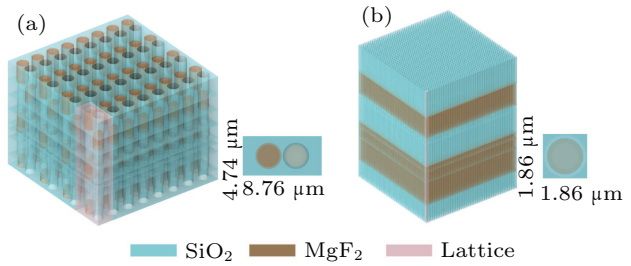


Fig. 3. Designed metamaterials for radiative cooling. (a) The selective radiative cooler. The right part is the top view of the rectangular primitive cell in plane whose length and width are 8.76 μm and 4.74 μm. The detail of the selective radiative cooler could be found in Table 1. (b) The broadband radiative cooler. The right part is the top view of the square primitive cell in plane which has a width of 1.86 μm. The detail of the broadband radiative cooler could be found in Table 1. The metamaterials are featuring periodic circular holes of different radii. The cyan layers are the multi-layers of SiO_2. The brown circulars are MgF_2. And the pink lattice presents the primitive cell of the radiative cooler.

Table 1. The structure information of the selective radiative cooler. The primitive cell in plane is a rectangular 4.74 μm × 8.76 μm. The thickness is the thickness of the SiO_2 layer. The center of the rectangular is set as the origin of coordinates. The center position is the center of the cylinder in plane. The radius is the radius of the cylinder. The filled material is the material of the cylinder of each layer.

No.	Thickness (μm)	Center position (μm)	Radius (μm)	Filled material
1	4.90	(0, −1.52) (0, 1.52)	1.45	air MgF_2
2	4.11	(0, −1.52) (0, 1.52)	1.25	MgF_2 air
3	3.71	(0, −1.52) (0, 1.52)	1.20	MgF_2 MgF_2
4	0.41	(0, −1.52) (0, 1.52)	1.27	air air
5	3.50	(0, −1.52) (0, 1.52)	1.40	MgF_2 air
6	1.57	(0, −1.52) (0, 1.52)	1.24	air MgF_2
7	2.24	(0, −1.52) (0, 1.52)	1.44	air air
8	4.72	(0, −1.52) (0, 1.52)	1.35	MgF_2 MgF_2
9	2.77	(0, −1.52) (0, 1.52)	1.16	air MgF_2
10	0.07	(0, −1.52) (0, 1.52)	1.38	air air

Based on the RCWA, we calculate the spectrum of the selective radiative cooler, as shown by the orange curve in Fig. 4. It is better than the SiO_2 and MgF_2 materials in the range of 8–13 μm. The absorptivity/emissivity near the 9 μm

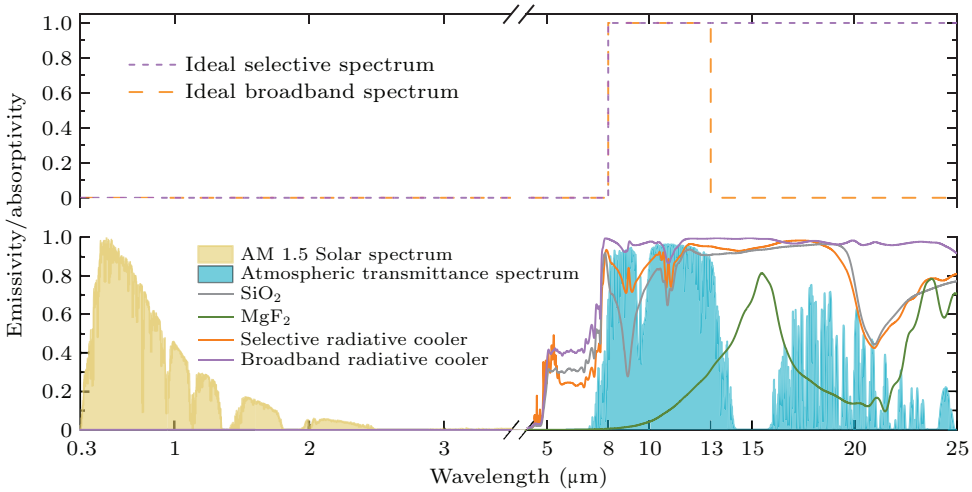


Fig. 4. Emissivity spectrum versus wavelength. The purple dot line and orange dash line are the spectrums of the ideal selective and broadband radiative coolers, respectively. The calculated spectra of SiO_2, MgF_2, designed selective radiative cooler and designed broadband radiative cooler are presented by gray, green, orange, purple lines, respectively. In the background, the AM 1.5 solar spectrum and atmospheric transmittance spectrum are presented by yellow and cyan areas, respectively.

is less than 0.3 for SiO_2 with gray curve, and close to 0 for MgF_2 with green curve. After optimizing the structure parameters of the selective radiative cooler, its emissivity around 9 μm remarkably exceeds 0.7. Assuming the ambient temperature being 300 K, we can obtain the cooling power of the selective radiative cooler at different conductive and convective heat exchange coefficients h of 0, 5 and 10 $W{\cdot}m^{-2}{\cdot}K^{-1}$, respectively, corresponding to the solid black line, blue dash line and orange dot line shown in Fig. 5(a). The refrigeration power $P_c(T_{amb})$ could reach 119 W/m^2 at the ambient temperature. When the cooling power drops to 0, the temperature of the cooler and the ambient reach equilibrium, and then the radiative cooler reaches its cooling limit. Without considering the coefficient of conductive and convective heat exchange ($h = 0$), the steady-state temperature T_{steady} of the selective radiative cooler could reach 265.5 K, which is 34.5 K lower than the ambient temperature.

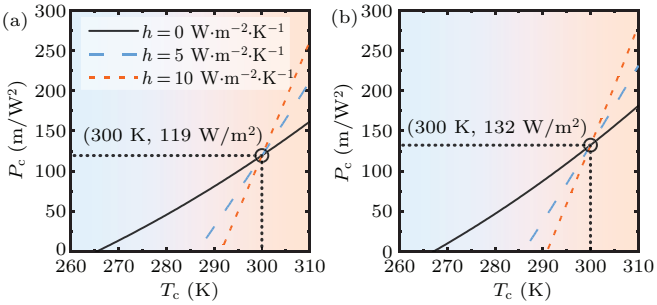


Fig. 5. Radiative cooling power versus the temperature of radiative cooler. (a) Net cooling power versus the temperature of the designed selective radiative cooler. (b) Net cooling power versus the temperature of the designed broadband radiative cooler. The ambient temperature T_{amb} is 300 K. The solid black line, blue dash line and orange dot line present the different combined heat conduction and heat convection coefficients h of 0, 5 $W{\cdot}m^{-2}{\cdot}K^{-1}$ and 10 $W{\cdot}m^{-2}{\cdot}K^{-1}$, respectively. When the temperature of the radiative cooler is equal to the ambient temperature 300 K, the net cooling powers of the designed selective and broadband radiative cooler are 119 W/m^2 and 132 W/m^2, respectively corresponding to the black empty circles.

Table 2. The structure information of the broadband radiative cooler. The primitive cell in plane is a square 1.86 μm×1.86 μm. The thickness is the thickness of the SiO_2 layer. The center of the square is set as the origin of coordinates. The center position is the center of the cylinder in plane. The radius is the radius of the cylinder. The filled material is the material of the cylinder of each layer.

No.	Thickness (μm)	Center position (μm)	Radius (μm)	Filled material
1	11.02	(0, 0)	0.92	air
2	8.74	(0, 0)	0.91	air
3	16.68	(0, 0)	0.76	MgF_2
4	4.38	(0, 0)	0.56	air
5	16.77	(0, 0)	0.82	air
6	4.37	(0, 0)	0.82	MgF_2
7	7.90	(0, 0)	0.76	MgF_2
8	17.44	(0, 0)	0.74	MgF_2
9	10.51	(0, 0)	0.87	air
10	2.31	(0, 0)	0.90	air

Since the ideal broadband radiative cooler has higher cooling efficiency than the ideal selective radiative cooler when its temperature is higher than or equal to the ambient temperature. We also design a broadband radiative cooler with the goal of 1 emissivity in the 8–25 μm range and zero emissivity otherwise, as shown in Fig. 3(b) and Table 2. The optimized structure is 10 layers of SiO_2. The thicknesses are 11.02, 8.74, 16.68, 4.38, 16.77, 4.37, 7.90, 17.44, 10.51 and 2.31 μm from top to bottom. The shape of the primitive cell in plane is 1.86 μm×1.86 μm with $p4m$ plane group. The filled cylinders are fixed at (0, 0), and the radii of the MgF_2/air cylinders are 0.925, 0.91, 0.76, 0.56, 0.82, 0.82, 0.76, 0.74, 0.87, 0.90 μm, respectively.

The calculated spectrum of the broadband radiative cooler is the purple curve in Fig. 4. Near the wavelength of 21 μm, the emissivity of SiO_2 material is about 0.45, and the emissivity of MgF_2 material is approximately 0.15. Similarly, the emissivity of the designed broadband radiative cooler is pushed to nearly 1 through our optimization, and the emissivity in the range of 8–13 μm is also close to 1. When the ambient temperature is fixed at 300 K, the broadband cooler has a cooling power $P_c(T_{amb})$ of 132 W/m^2 at the ambient temperature as shown in Fig. 5(b), which is 13 W/m^2 higher than that of the selective radiative cooler. We note that, when the temperature of the cooler is higher than or equal to the ambient temperature, the broadband radiative cooler is more effective than the selective one. However, after a sufficiently long time, the selective cooler ultimately reaches a steady state temperature T_{steady} (265.5 K) 1.7 K lower than the broadband one for small h ($h \approx 0$).

As shown in Table 3, our selective and broadband coolers show a high radiative cooling performance. Their net radiative cooling powers and steady-state temperatures are superior than or at least approximate with the previously reported cutting-edge radiative coolers.[3,7,22,41,51] Moreover, distinct with these results, our work particularly provides a general designing schematic of the radiative cooling metamaterials without much a priori knowledge or experience.

Table 3. The net cooling power at the ambient temperature and the temperature decrease at the steady state of the designed material. $P_c(T_{amb})$ is the net cooling power of the material without the non-radiative heat-exchanges at the ambient temperature. $T_{amb} - T_{steady}$ is the maximum temperature decrease where the net cooling power vanishes.

Material	$P_c(T_{amb})$ ($W \cdot m^{-2}$)	$T_{amb} - T_{steady}$ (K)
Selective cooler	**119**	**34.5**
Broadband cooler	**132**	**32.8**
Multilayer (HfO_2, SiO_2)[3]	38	19.5
Multilayer (HfO_2, MgF_2, SiC)[41]	46	23.4
Metamaterial $(quartz, SiC, MgF_2, TiO_2)$[7]	105	–
Metamaterial (TPX, SiO_2)[22]	93	–
Metamaterial (SiO_2, Ag)[51]	134	28.7

5. Conclusion

In summary, we have developed and summarized a kind of method, which is combining with symmetries of 17 plane groups, PSO algorithm and RCWA theory to design and optimize the spectrum of photonic metamaterials for radiative cooling. On the basis of this method, we effectively design two multilayer metamaterials formed by 10-layer SiO_2 with different cylindrical holes filled with MgF_2 and air for the selective and broadband radiative cooling devices, respectively. Moreover, the selective and broadband radiative coolers could achieve 119 W/m^2 and 132 W/m^2 net radiative cooling power at 300 K, respectively. The results show that the combination of the two materials with poor radiative cooling performance could achieve a high-performing radiative cooler. Due to the effectiveness of designing photonic metamaterials for radiative cooling by PSO, the method has the great potential applications in discovery of high-performing photonic, acoustic and thermal metamaterials. Furthermore, the relationship between the symmetry and radiative cooling could be explored by constraining the spatial symmetry of structures during the PSO evolution process in the future work.

Acknowledgements

Project supported by the National Natural Science Foundation of China (Grant No. 11935010) and the Opening Project of Shanghai Key Laboratory of Special Artificial Microstructure Materials and Technology.

References

[1] Zhao D, Aili A, Zhai Y, Xu S, Tan G, Yin X and Yang R 2019 *Appl. Phys. Rev.* **6** 021306
[2] Yu X, Chan J and Chen C 2021 *Nano Energy* **88** 106259
[3] Raman A P, Anoma M A, Zhu L, Rephaeli E and Fan S 2014 *Nature* **515** 540
[4] Fan S and Li W 2022 *Nat. Photon.* **16** 182
[5] Peng J, Tang G, Wang L, Macêdo R, Chen H and Ren J 2021 *ACS Photon.* **8** 2183
[6] Liang J, Wu J, Guo J, Li H, Zhou X, Liang S, Qiu C W and Tao G 2022 *Natl. Sci. Rev.* **10** nwac208
[7] Rephaeli E, Raman A and Fan S 2013 *Nano Lett.* **13** 1457
[8] Hossain M M and Gu M 2016 *Adv. Sci.* **3** 1500360
[9] Granqvist C and Hjortsberg A 1980 *Appl. Phys. Lett.* **36** 139
[10] Granqvist C and Hjortsberg A 1981 *J. Appl. Phys.* **52** 4205
[11] Berdahl P, Martin M and Sakkal F 1983 *Int. J. Heat Mass Transf.* **26** 871
[12] Orel B, Gunde M K and Krainer A 1993 *Sol. Energy* **50** 477
[13] Suryawanshi C N and Lin C T 2009 *ACS Appl. Mater. Interfaces* **1** 1334
[14] Gentle A R and Smith G B 2010 *Nano Lett.* **10** 373
[15] Catalanotti S, Cuomo V, Piro G, Ruggi D, Silvestrini V and Troise G 1975 *Sol. Energy* **17** 83
[16] Johnson T 1975 *Sol. Energy* **17** 173
[17] Zhao B, Hu M, Ao X, Xuan Q and Gang P 2018 *Sol. Energy Mater. Sol. Cells* **178** 266
[18] Hossain M M, Jia B and Gu M 2015 *Adv. Opt. Mater.* **3** 980
[19] Zou C, Ren G, Hossain M M, Nirantar S, Withayachumnankul W, Ahmed T, Bhaskaran M, Sriram S, Gu M and Fumeaux C 2017 *Adv. Opt. Mater.* **5** 1700460
[20] Kou J l, Jurado Z, Chen Z, Fan S and Minnich A J 2017 *ACS Photon.* **4** 626
[21] Zhu L, Raman A, Wang K X, Anoma M A and Fan S 2014 *Optica* **1** 32
[22] Zhai Y, Ma Y, David S N, Zhao D, Lou R, Tan G, Yang R and Yin X 2017 *Science* **355** 1062
[23] Wan P, Wen X, Sun C, Chandran B K, Zhang H, Sun X and Chen X 2015 *Small* **11** 5409
[24] Xiong W, Liu H, Chen Y, Zheng M, Zhao Y, Kong X, Wang Y, Zhang X, Kong X and Wang P 2016 *Adv. Mater.* **28** 7167
[25] Zhu H, Li Q, Tao C, Hong Y, Xu Z, Shen W, Kaur S, Ghosh P and Qiu M 2021 *Nat. Commun.* **12** 1805
[26] Bijarniya J P, Sarkar J and Maiti P 2020 *Renew. Sust. Energ. Rev.* **133** 110263
[27] Mandal J, Fu Y, Overvig A C, Jia M, Sun K, Shi N N, Zhou H, Xiao X, Yu N and Yang Y 2018 *Science* **362** 315
[28] Lu X, Xu P, Wang H, Yang T and Hou J 2016 *Renew. Sust. Energ. Rev.* **65** 1079
[29] Santamouris M and Feng J 2018 *Buildings* **8** 168
[30] Chen L, Zhang K, Ma M, Tang S, Li F and Niu X 2020 *Build. Simul.* **13** 1165
[31] Li W, Li Y and Shah K W 2020 *Sol. Energy* **207** 247
[32] Li X, Xie W, Sui C and Hsu P C 2020 *ACS Mater. Lett.* **2** 1624
[33] Zhu L, Raman A P and Fan S 2015 *Proc. Natl. Acad. Sci. USA* **112** 12282
[34] Li W, Shi Y, Chen K, Zhu L and Fan S 2017 *ACS Photon.* **4** 774
[35] Hsu P C, Song A Y, Catrysse P B, Liu C, Peng Y, Xie J, Fan S and Cui Y 2016 *Science* **353** 1019
[36] Lan X, Wang Y, Peng J, Si Y, Ren J, Ding B and Li B 2021 *Mater. Today Phys.* **17** 100342
[37] Peng Y and Cui Y 2020 *Joule* **4** 724
[38] Xia Z, Zhang Z, Meng Z, Ding L and Yu Z 2019 *ACS Appl. Mater. Interfaces* **11** 33941
[39] Raman A P, Li W and Fan S 2019 *Joule* **3** 2679
[40] Dong M, Zhang Z, Shi Y, Zhao X, Fan S and Chen Z 2020 *Nanoscale Microscale Thermophys. Eng.* **24** 43
[41] Shi Y, Li W, Raman A and Fan S 2018 *ACS Photon.* **5** 684
[42] Long Y, Ren J, Li Y and Chen H 2019 *Appl. Phys. Lett.* **114** 181105
[43] Chen J, Peng J, Yang C, Dun X, Cheng X, Chen H and Ren J 2021 *Appl. Phys. Lett.* **119** 114102
[44] Long Y, Ren J and Chen H 2020 *Phys. Rev. Lett.* **124** 185501
[45] Tan Y T, Wang L Q, Wang Z, Peng J and Ren J 2021 *Chin. Phys. B* **30** 036301
[46] Yan S, Wang Y, Gao Z, Long Y and Ren J 2021 *Chin. Phys. Lett.* **38** 027301
[47] Molesky S, Lin Z, Piggott A Y, Jin W, Vucković J and Rodriguez A W 2018 *Nat. Photon.* **12** 659
[48] Jiang J, Chen M and Fan J A 2021 *Nat. Rev. Mater.* **6** 679
[49] Chen Z and Segev M 2021 *eLight* **1** 2
[50] Chae D, Kim M, Jung P H, Son S, Seo J, Liu Y, Lee B J and Lee H 2020 *ACS Appl. Mater. Interfaces* **12** 8073
[51] García-Esteban J, Bravo-Abad J and Cuevas J 2021 *Phys. Rev. Appl.* **16** 064006
[52] Zhang Z, Dai Y and Ma C 2021 *Opt. Commun.* **500** 127323
[53] Naghshine B B and Saboonchi A 2018 *Opt. Commun.* **410** 416
[54] Huang Y, Pu M, Zhao Z, Li X, Ma X and Luo X 2018 *Opt. Commun.* **407** 204
[55] Kim S, Shang W, Moon S, Pastega T, Lee E and Luo T 2022 *ACS Energy Lett.* **7** 4134
[56] Guo J, Ju S, Lee Y, Gunay A A and Shiomi J 2022 *Int. J. Heat Mass Transf.* **195** 123193
[57] Aydin K, Ferry V E, Briggs R M and Atwater H A 2011 *Nat. Commun.* **2** 517
[58] Hossain M M, Jia B and Gu M 2015 *Adv. Opt. Mater.* **3** 1047
[59] Zhang W W, Qi H, Sun A T, Ren Y T and Shi J W 2020 *Opt. Express* **28** 20609
[60] Wang Y, Lv J, Zhu L and Ma Y 2010 *Phys. Rev. B* **82** 094116
[61] Oganov A R and Glass C W 2006 *J. Chem. Phys.* **124** 244704
[62] Kennedy J and Eberhart R 1995 *Proceedings of ICNN'95 - International Conference on Neural Networks*, November 27–December 1, 1995, Perth, WA, Australia, p. 1942
[63] Poli R, Kennedy J and Blackwell T 2007 *Swarm Intell.* **1** 33
[64] Lyakhov A O, Oganov A R and Valle M 2010 *Comput. Phys. Commun.* **181** 1623
[65] Lyakhov A O, Oganov A R, Stokes H T and Zhu Q 2013 *Comput. Phys. Commun.* **184** 1172
[66] Liu V and Fan S 2012 *Comput. Phys. Commun.* **183** 2233
[67] Zhan Z H, Zhang J, Li Y and Chung H S H 2009 *IEEE Trans. Syst. Man Cybern. Part B-Cybern.* **39** 1362
[68] Shi Y and Eberhart R 1998 *IEEE International Conference on Evolutionary Computation Proceedings. IEEE World Congress on Computational Intelligence* (Cat. No. 98TH8360), May 4–9, 1998, Anchorage, AK, USA, p. 69
[69] Wu D, Liu C, Xu Z, Liu Y, Yu Z, Yu L, Chen L, Li R, Ma R and Ye H 2018 *Mater. Des.* **139** 104